

Methods to Induce Chronic Ocular Hypertension: Reliable Rodent Models as a Platform for Cell Transplantation and Other Therapies

Cell Transplantation
2018, Vol. 27(2) 213–229
© The Author(s) 2018
Reprints and permission:
sagepub.com/journalsPermissions.nav
DOI: 10.1177/0963689717724793
journals.sagepub.com/home/cil


Ashim Dey¹, Abby L. Manthey², Kin Chiu^{2,3,4}, and Chi-Wai Do¹

Abstract

Glaucoma, a form of progressive optic neuropathy, is the second leading cause of blindness worldwide. Being a prominent disease affecting vision, substantial efforts are being made to better understand glaucoma pathogenesis and to develop novel treatment options including neuroprotective and neuroregenerative approaches. Cell transplantation has the potential to play a neuroprotective and/or neuroregenerative role for various ocular cell types (e.g., retinal cells, trabecular meshwork). Notably, glaucoma is often associated with elevated intraocular pressure, and over the past 2 decades, several rodent models of chronic ocular hypertension (COH) have been developed that reflect these changes in pressure. However, the underlying pathophysiology of glaucoma in these models and how they compare to the human condition remains unclear. This limitation is the primary barrier for using rodent models to develop novel therapies to manage glaucoma and glaucoma-related blindness. Here, we review the current techniques used to induce COH-related glaucoma in various rodent models, focusing on the strengths and weaknesses of the each, in order to provide a more complete understanding of how these models can be best utilized. To so do, we have separated them based on the target tissue (pre-trabecular, trabecular, and post-trabecular) in order to provide the reader with an encompassing reference describing the most appropriate rodent COH models for their research. We begin with an initial overview of the current use of these models in the evaluation of cell transplantation therapies.

Keywords

rodent models, glaucoma, chronic ocular hypertension

Introduction

Glaucoma is physiologically characterized by elevated intraocular pressure (IOP), progressive retinal ganglion cell (RGC) death, loss of RGC axons, optic nerve excavation, and visual field loss that can lead to irreversible blindness¹. Although elevated IOP is considered the major risk factor^{2–5}, progressive loss of the RGCs has been shown to continue even when the IOP is adequately controlled via medication or surgery^{6,7}. To better understand the glaucomatous RGC degeneration, a large body of research has focused on the pathophysiological mechanisms thought to be involved, including the role of increased oxidative stress and free radicals, the release of neurotransmitters (e.g., nitric oxide and glutamate), the depletion of neurotrophins and growth factors, and the initiation of apoptosis^{8–13}. There has also been increased interest in the use of cell transplantation therapeutics to treat these mechanisms via a single intervention (e.g., cell graft) which could provide long-lasting protection

¹ School of Optometry, The Hong Kong Polytechnic University, Hung Hom, Kowloon, Hong Kong, China

² Laboratory of Retina Brain Research, Department of Ophthalmology, LKS Faculty of Medicine, The University of Hong Kong, Hong Kong, China

³ Research Centre of Heart, Brain, Hormone and Healthy Aging, The University of Hong Kong, Hong Kong, China

⁴ State Key Laboratory of Brain and Cognitive Sciences, The University of Hong Kong, Hong Kong, China

Submitted: June 19, 2016. Revised: March 25, 2017. Accepted: April 23, 2017.

Corresponding Author:

Kin Chiu, Rm. 410, Hong Kong Jockey Club Building for Interdisciplinary Research, 5 Sassoon Road, Pokfulam, Hong Kong, China; Chi-Wai Do, School of Optometry, The Hong Kong Polytechnic University, Yuk Choi Road, Hung Hom, Kowloon, Hong Kong, China.
Emails: datwai@hku.hk; chi-wai.do@polyu.edu.hk



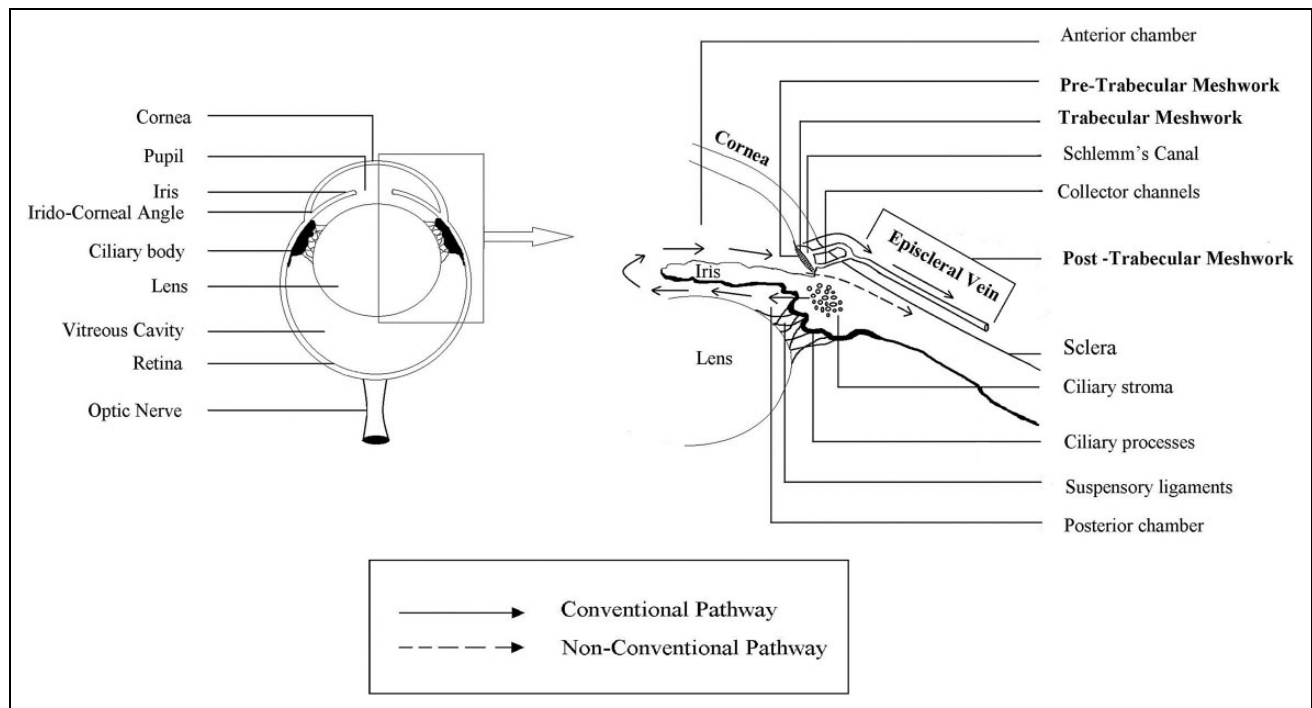


Figure 1. Schematic diagram illustrating the structure of whole eye (left) and anterior segment (right). During the conventional outflow pathway, aqueous humor is produced by the ciliary body and it flows from the posterior chamber through the pupil into the anterior chamber (shown by continuous lines with arrowheads). It then flows out through the trabecular meshwork into Schlemm's canal and is subsequently absorbed into the episcleral veins via the collector channels. In the unconventional outflow pathway, aqueous humor flows out from anterior chamber through the face of the ciliary body and iris root to the ciliary muscle and suprachoroidal space to either veins in the choroid and sclera or through scleral pores to episcleral tissue (shown by dashed lines and arrowheads).

during glaucoma pathogenesis or other chronic ocular diseases^{14–16}. Indeed, several preclinical studies have reported positive outcomes using cell transplantation in animal glaucoma models. For example, implantation of bone marrow mesenchymal stem cells (BM-MSCs) reduces IOP in a chronic ocular hypertension (COH) rodent model in addition to significantly enhancing the survival of RGCs compared to the control animals¹⁷. Similarly, implantation of induced pluripotent stem cells in the anterior chamber (AC) of 4-mo-old transgenic-Y437H myocilin mutant mice (Tg-MYOC^{Y437H}) has been shown to restore trabecular meshwork (TM) function and stabilize IOP as well as increase RGC survival compared to control animals for 9 wk post-implantation¹⁸. Several other studies have also reported neuroprotective effects following intravitreal injection of BM-MSCs in a number of inducible COH rodent models, including models using laser treatment^{19,20}, hyaluronic acid (HA) injection²¹, and intra-cameral injections of transforming growth factor- β 1 (TGF- β) for 0 to 35 d²². Intravitreal injection of dental pulp stem cells also appears to protect structural and functional loss of RGCs in induced COH rodent glaucoma²² as well as in a rodent axotomy model²³. Apart from the injection of pluripotent and/or mesenchymal cells, other cell transplantation therapies involving glucagon-like peptide-1 have also been shown to protect RGCs and their axons in an optic nerve crush model²⁴. These studies indicate

that cell transplantation has the potential to play a favorable hypotensive and neuroprotective role against glaucoma by reducing IOP, enhancing RGC survival and outgrowth, and/or altering the RGC microenvironment. While development of neuroprotective and/or neuroregenerative therapeutic strategies is an essential avenue of research, the majority of these treatments have not yet been tested in clinical or preclinical studies. Fortunately, various animal models have been established that mimic the ocular changes associated with glaucoma^{25–27}, allowing investigation of the underlying pathophysiology of this disease and the testing of treatment efficacy.

While the anatomy and physiology of rodent eyes differ in some ways to human eyes^{28–30}, inducible rodent systems are preferred for several reasons, including the ethics of their experimental use, shorter life span, and cost-effectiveness^{29,31–37}. It has been suggested that the conventional outflow pathway in the mouse eye is similar to that of primate eye as it has a continuous Schlemm's canal and lamellated TM³⁸. Furthermore, the changes observed during human glaucoma can also be reasonably mimicked in rodents. This seems to be particularly true in regard to the lamina cribrosa changes in the glaucomatous optic nerve head²⁸. The aqueous humor is produced by the ciliary body in the rat eye, flows through the TM, and is collected in Schlemm's canal located in the angle of the AC in a manner similar to that

observed in humans³¹. The aqueous humor then enters the venous plexus through collector channels in the limbal region, allowing it to drain from the eye through the episcleral drainage veins³². It is the dynamic balance of aqueous humor inflow and outflow that effectively maintains physiological IOP levels in both species (Figure 1).

In order to mimic the glaucoma-inducing changes in IOP, various methods have been utilized to block the outflow of aqueous humor in rodents^{25,26}. Although a vast amount of research using these models exists, very few articles have directly compared the physiological attributes of these models to human glaucoma. In this review, we have summarized the most prevalent experimental methods utilized to induce COH in rodents, focusing on how they can be most effectively used in translational research. This review can also function as a guide for researchers to determine the appropriate glaucoma rodent model for their own research needs. To this end, the methods described here can be classified into 3 primary groups: (Pre-TM), trabecular, and post-trabecular (Post-TM) obstruction of the outflow³⁹ as shown in Figure 1.

Pre-TM Models

AC Injection of Obstructive Substances

Outflow obstruction is often physically induced before the aqueous humor passes through the TM. HA, microspheres/microbeads, and magnetic microbeads have been used as occlusion sources. Once injected into the AC, they cannot pass through the TM due to their size and subsequently impede outflow.

Injection of HA. HA is a naturally occurring glycosaminoglycan polysaccharide that is widely distributed throughout the human body in tissues such as the skin, cartilage, hair, and eyes⁴⁰. In the eye, HA is primarily localized to the aqueous humor, vitreous humor, and TM, where it appears to play an important role in the migration and maintenance of the extracellular matrix⁴⁰⁻⁴². Furthermore, this polysaccharide also creates a gradient pressure between the AC and the aqueous outflow pathways⁴³. Thus, an optimal concentration of HA is required to maintain normal outflow levels throughout the TM.

Interestingly, the concentration of HA in the aqueous humor isolated from patients with primary open angle glaucoma was found to be significantly lower (0.32 $\mu\text{g}/\text{mL}$) than controls (0.61 to 2.56 $\mu\text{g}/\text{mL}$)⁴⁴, whereas the concentration in the aqueous humor of exfoliation subjects was significantly higher (7.8 $\mu\text{g}/\text{mL}$) than controls⁴⁵. In fact, it has been noted that injection of HA during various intraocular surgeries, including cataract surgery⁴⁶⁻⁴⁸, appears to cause a transient increase in IOP among 81% of operated eyes (>10 mmHg)⁴⁹.

The effect of HA on IOP has also been utilized to induce changes in a number of animal models. Benozzi et al.⁵⁰ were the first to inject a 25 μL aliquot of HA (10 $\mu\text{g}/\text{mL}$) into the

AC of an anesthetized rat. In this study, 1 single injection was found to raise the IOP 2-fold after 24 h, and this increase sustained for 8 d. Weekly injection could also be used to maintain the elevated IOP for up to 10 wk⁵¹. Notably, intracameral HA injection also appears to cause a significant loss of RGCs (40%) as well as functional changes compared with the controls 10 wk after injection⁵¹.

Injection of latex microspheres. Microspheres are spherical microbeads in the colloidal size range (diameter 0.02 to 15 μm) that are composed of an amorphous polymer such as polystyrene. They can also be loaded with a variety of dyes (e.g., fluorescein) that can be easily traced inside tissues via fluorescence microscopy. In this way, microspheres have been used for various experiments involving blood flow tracing and drug delivery.

Weber and Zelenak⁵² were the first to use injected microspheres to induce COH in the eyes of rhesus monkeys. Their experiments were followed by those of Urcola et al.⁵³ that focused on using injected microspheres to similarly induce COH in rat eyes. In these experiments, it appears that weekly injections of 2 to 4 $\times 10^5$ latex microspheres (diameter 10 μm) in 20 μL of a sterile aqueous solution (0.15 M NaCl, 0.02% Tween 20) into the AC using a 30-gauge needle effectively blocked the TM, causing a subsequent elevation in IOP. Similarly, a combination of 10 μL of microspheres (1 to 2 $\times 10^5$) with 10 μL of 2% hydroxypropylmethylcellulose (HPM) injected weekly into the AC also increases IOP, but this increase occurs earlier (6 wk) compared with injections of microspheres alone (9 wk) and can be sustained for 30 wk. While mechanical obstruction itself is a simple process, it remains unclear why there is a delay in the elevation of IOP. Researchers have speculated that this phenomenon could be due to species differences and/or the repeated use of general anesthesia⁵³. Notably, the peak IOP in both studies was observed at week 27, when the IOP was 1.69-fold and 1.98-fold higher than the controls, respectively. Morphologically, loss of the RGCs was noted in 23.1% \pm 2.1% of the animals injected with microspheres alone, while 27.2% \pm 2.1% had RGC death in the microsphere and HPM group after 24 wk of induced IOP elevation⁵³.

More recently, Sappington et al.⁵⁴ also used polystyrene microbeads to block the TM and produce COH in both brown Norway rats and C57BL/6 mice. In the rats, 15- μm -diameter polystyrene microbeads were injected at a concentration of 1 $\times 10^6$ beads/mL via micropipette in volumes ranging from 2.5 to 7 μL in order to evaluate the effect of volume on elevated IOP. Single injections of these microbeads were observed to induce a 21% to 34% increase in IOP compared to the controls within the first 2 wk. An additional injection after this initial 2 wk was also shown to maintain this IOP increase for an additional 6 wk. Notably, there was a significant difference in the induced IOP in the rat eyes after injection of 2.5, 5, and 7 μL , with the 2 higher injection volumes producing similar elevations in IOP. In the mice, a 1 μL volume of 15 μm diameter microbeads injected into

the AC was observed to produce a 30% increase in IOP compared with the controls and persisted for at least 3 wk. There was also a significant loss of axons and induced gliosis along with degeneration and disorganization of the optic nerve in both rats and mice 4 to 5 wk after the initial injection. Recent experiments conducted by Cone-Kimball et al.⁵⁵ also highlighted the effects of mouse strain on IOP elevation post-microbead injection, indicating that this technique involves a high level of variability depending on genetic background, injection volume, and so on.

Injection of paramagnetic microspheres. Unlike latex microspheres, paramagnetic microspheres are typically composed of polystyrene and uniformly coated with a biocompatible ferrosulfuric oxide complex that allows them to respond to a magnet or magnetic field. Following exposure to a magnetic field, these particles retain their magnetic properties and can be demagnetized and remagnetized repeatedly and reproducibly. Paramagnetic microspheres have also been shown to be nontoxic and do not have any associated systemic side effects⁵⁶. Thus, these particles are ideal for drug delivery, whereby various medicines can be enclosed in the polystyrene bead, injected into the blood stream, and effectively directed to the target site with the help of a magnet.

In addition to drug delivery, Samsel et al.⁵⁷ have used this technique to evenly distribute the microbeads into the AC of rats to consistently induce COH. With this method, 10 to 20 μL aliquots of 30 mg/mL ferromagnetic microspheres (5 μm in diameter) are injected into the AC with a 30-gauge needle. After injection, the microbeads can be spread evenly around the iridocorneal angle from the site of injection with a magnet. Using this technique, a single injection was observed to induce a sustained increase in IOP greater than 5 mmHg for 12 d, while 3 injections resulted in 6 wk of prolonged IOP elevation and a 36% loss of RGCs. A similar study using the same model reported axonal loss (80%) 4 wk after injection, a result which may reflect a more acute insult to the retina rather than COH⁵⁸. Recently, Bunker et al.⁵⁹ used a modified version of this procedure using a circular magnet placed around the rat eye prior to injection of the magnetic microbeads (diameter 8.0 μm). Using this technique, they observed an even distribution of microbeads around the iridocorneal angle as well as a sustained increase in IOP (40.5 ± 2.8 mmHg) compared to control eyes (19.7 ± 0.3 mmHg) for 18 d after a single injection. This increase also caused a subsequent change in RGC death, with the level of apoptosis increasing approximately 15-fold compared with the controls⁵⁹.

General Points Concerning Pre-TM Models

Each of these pre-trabecular obstruction methods is inexpensive, easy to perform, and temporarily blocks the TM to increase IOP. They have been used extensively for evaluating drug delivery and to investigate changes in outflow and IOP. Furthermore, these methods also have minimal

ischemia associated with them, as they do not block blood flow to or from the eye. However, although useful and effective, multiple injections are needed in order to sustain a higher IOP, which is both time and labor intensive. This need for multiple injections stems from the basic concept of physical obstruction to induce COH, whereby the beads get stuck in the intracellular spaces of the TM causing impairment of aqueous humor outflow and increased IOP. However, for these effects to be considered chronic, the obstruction is by nature transient, with small clumps of the microspheres gathering to gradually obstruct drainage. This necessitates the use of multiple injections in order to produce a sustained increase in IOP. Furthermore, elevation of IOP also causes widening of the paracellular spaces, which may increase the space between the cells allowing greater aqueous humor outflow and flow through of the beads themselves. Hence, additional beads are required to completely block the TM⁵². These issues with retaining the obstructive substance, be it beads or HA, after injection may also result in variable or inconsistent changes in IOP, which may limit the practical use of these models. In fact, several studies using microbeads to induce COH reported that the diameter and volume injected into the AC significantly influences the resulting change in IOP. Thus, several researchers have tried to minimize the effects of these variables by using viscous substances and/or different compositions of bead size (Table 1).

Moreover, in addition to being time and labor intensive, multiple injections increase the chance of infection and possible downstream changes in ocular function not associated with COH. Indeed, multiple injections increase the likelihood of injury to the cornea, lens, and retina as well as changes in aqueous-vitreous or blood-ocular barrier integrity⁶⁶. Moreover, the localization of the obstruction within the AC is also difficult to control. For example, if beads aggregate in the pupillary zone, they can obscure the visual axis, compromise fundoscopic monitoring of optic nerve damage, or cause leakage of the substance into the eye.

Taken together, while these pre-trabecular models have a number of advantages, additional work may be necessary to develop consistent results for preclinical trials.

TM Models

Laser Treatments

Unlike the pre-trabecular methods, laser photocoagulation (LPC) blocks the outflow of the aqueous humor by destroying the TM tissue itself, and TM tissues can be burned using an argon laser to induce COH⁶⁷. Lasers are forms of light that can hold a huge amount of energy, which in this context are focused to burn the target tissues. Argon lasers, for example, have a spectral range with emission peaks at wavelengths within the visible light range (488 and 514 nm) and have been extensively used for the treatment of various ocular diseases, including diabetic retinopathy, glaucoma, and premacular hemorrhage⁶⁸.

Table 1. Effect of Volume and Bead Size on the Ability of an Injected Substance to Elevate IOP.

Injected Substance	Species	Bead Size (µm)	Total Volume (µL)	Duration (wk)	C_Mean IOP (mmHg)	G_Mean IOP (mmHg)	ERG	RGCs Loss %	Axon Loss %	Remarks	References
HA	Wistar rats		25	1*	11.9 ± 0.7	15.5 ± 1.0				*8 d, Weekly repeated injection can sustain IOP for 10 wk	50
Latex microspheres	SD rats	10	20	30	23.06 ± 0.8	28.1 ± 0.7		23.1		Weekly 9 injections required to sustain high IOP	53
Latex microspheres + HPM		10	20 (10 + 10)	30	23.06 ± 0.8	31.1 ± 0.6		27.2		Weekly 6 injections required to sustain high IOP	
Polystyrene beads	BN rats	15	2.5	2**	21.4 ± 0.95	26.9				**13 d, ***10 d	54
		15	5	2	21.3 ± 1.3	28.8					
		15	7	1.5***	21.3 ± 0.96	29.7					
HA + Polystyrene beads	C57BL/6 mice	15	1	3	15.3 ± 0.08	20.0 ± 0.8		5.2	6.5	#8-wk-old rats, 13.6% increase in AXL postbred injection	60
	C57BL6 (younger#/ older###)	6	5 (3 + 2)	12	9.8 ± 1.0	14.4 ± 4.0		4.1	0.1	##8-mo-old rats, 8.3% increase in AXL postbred injection	
		6	5 (3 + 2)	12	11.2 ± 0.8	16.4 ± 2.5		4.1	13.9	8.7% increase in AXL postbred injection	
	DBA/2J mice	6	5 (3 + 2)	12	10.7 ± 0.9	13.0 ± 2.6		4.1	32	4.3% increase in AXL postbred injection	
	CD1 mice	6	5 (3 + 2)	12	10.3 ± 0.8	13.5 ± 3.2		20.1	31	4.3% increase in AXL postbred injection	61
Visco + Polystyrene beads	Mice*	6 + 1	5 (1 + 2 + 2)	6		15.3 ± 4.6			16	¥B6.Cg-Tg (Thyl-YFPH)2Jrs/J	62
	C57BL/6 mice	6	5 (3 + 2)	6	9.8 ± 1.1	18.6 ± 3.2		10	7	7% increase in AXL postinjection	
		6 + 1	5 (1 + 2 + 2)	6	10.2 ± 0.8	11.8 ± 2.0			42		
	CD1 mice	6	5 (3 + 2)	6	10.3 ± 1.8	21.6 ± 4.9			23		
		6 + 1	5 (1 + 2 + 2)	6	13.5 ± 1.4	12.9 ± 2.7					
		6 + 1	5 (2 + 1.5 + 1.5)	6	10.4 ± 0.9	15.6 ± 5.5	↓pSTR	11.2		Increase in AXL	63
Polystyrene beads	C57BL/6mice	6 + 1	5 (3 + 2)	12	12.3 ± 3.3						
Visco + Polystyrene beads	Wistar rats	6 + 10	15 (5 + 5 + 5)	6	11.4 ± 0.8	30.9 ± 3.2		34	25	Increase in AXL was not reported	64
HA + Polystyrene beads	C57BL/6mice	6 + 1	3 + 1.5	24	10.6 ± 2.8	13.1 ± 4.1	↓pSTR	14.4		Increase in AXL	65
Magnetic beads	BN rats	5	10 – 20	4	23.6 ± 0.4	29.4 ± 0.9		36.4		Weekly repeated injection (3)	57
	AS rats	5	20	4	24.59 ± 0.42	28.15 ± 4.37			80.3	Peak IOP 43.05 ± 2.33 at 1 wk	58

Abbreviations: IOP, intraocular pressure; C_Mean IOP, control eyes_mean IOP; G_Mean IOP, glaucoma eyes_mean IOP; ERG, electroretinogram; RGCs, retinal ganglion cells; HA, hyaluronic acid; HPM, hydroxypropylmethylcellulose; SD rats, Sprague-Dawley rats; BN rats, Brown-Norway rats; AS rats, Albino Swiss rats; AXL, axial length; pSTR, positive scotopic threshold response.

*,**,*** Represent the duration of sustained IOP elevation (in days/wk) for a single intervention.

Represents the age of the mice and * denotes the detail of the mutant mice.

COH induced by LPC of the TM was first demonstrated in rats by Ueda et al.⁶⁹. They injected 0.05 mL of Indian ink into the AC of rat eyes with a 30-gauge needle 1 wk prior to laser treatment. Indian ink consists of carbon particles which stick to the TM, creating a 0.2 mm wide black band in the limbal area. Then, when a 250 mW power laser is focused for 0.2 s (0.5 mm spot size) directly on the black band, the small carbon particles absorb the heat of laser and effectively damage/scar the TM. This damage results in the subsequent impairment of the aqueous outflow and a sustained increase in IOP for 4 wk following 3 consecutive laser treatments performed in 7 d intervals. Notably, the IOP was observed to decrease once the laser treatments were stopped. In addition to altering IOP, this method also produced glaucomatous optic nerve changes, including thinning of the nerve fiber layer, reduction of axons, and degeneration of the optic nerve. Ink injection alone did not affect IOP and was naturally eliminated from the tissue by 12 wk postinjection⁶⁹. Using similar methods, Park et al.⁷⁰ reported a 47% increase in IOP and a 51% loss of RGCs compared to contralateral eyes after 8 wk of laser treatments in Wistar rats. Levkovitch-Verbin et al.⁷¹ have also evaluated laser-induced changes in multiple ocular tissues, focusing on the TM with or without additional damage to the episcleral veins, in Wistar rats. They reported that TM-only laser treatments cause a significant increase in IOP and loss of RGCs (approximately 49%) after 9 wk. However, 76% of the eyes required an additional laser treatment on the TM to increasing the IOP significantly compared to controls. Their work is further discussed in the post-TM models section.

To establish a similar laser-induced COH model in mice, various methods have been evaluated. For example, Aihara et al.⁷² and Mabuchi et al.⁷³ previously demonstrated the applicability of this model for inducing COH in Black Swiss mice. In these studies, the mouse pupil was dilated with topical mydriasis, and the aqueous humor was aspirated to flatten the AC, bringing the root of iris closer to the peripheral cornea. Then, LPC was applied to the limbal area with a diode laser system (532 nm) to achieve angle closure (peripheral anterior synechia). This method produced a 1.3-fold rise in IOP for 6 wk after a single laser treatment. Compared to the contralateral eye, there was also a significant decrease in the optic nerve cross-sectional area (28%), mean axonal density (58%), and total number of axons (63%).

Viral Vector Treatment

Another emerging method for increased IOP in rodent models is the use of viral vectors, whereby injection into the AC or vitreous cavity results in viral gene transfer leading to the impairment of aqueous outflow and increased IOP⁷⁴. Shepard et al.⁷⁵ have reported that a single intravitreal or intracameral injection of a viral vector containing human TGF-2 into rat (5 μ L) or mouse (2 μ L) eyes caused a significant increase in IOP. This significant increase was noted after 4 d

of injection and was maintained for 12 d in rat eyes and 29 d in mouse eyes compared to their respective controls. Interestingly, the authors also observed that intravitreal injection in mice caused a prolonged effect compared to intracameral injection. Similarly, Buie et al.⁷⁶ reported a sustained 48 d increase in IOP following single intracameral injection of bone morphogenetic protein 2 in the eyes of Brown-Norway and Wistar rats which caused 31% to 34% loss of RGCs compared to the controls after 29 d of injection.

General Points Concerning TM Models

Although laser-induced destruction of the TM (Table 2) has many advantages, it also has various limitations. For example, laser treatment can alter TM pigmentation and repeated application may also prompt other complications, including dryness, corneal opacity, and cataract formation. These changes may in turn affect the technical aspects of the procedures, imaging quality, experimental outcomes, and/or cause higher mortality rates in the animals. Furthermore, one of the primary drawbacks of the LPC methods described here is that they require perforation of the cornea, which can increase the chances of infection and may affect IOP measurements made using tonometer devices as the corneal parameters are altered. Additionally, flattening of the AC can also cause variability in the IOP, possibly limiting the significance of the experiments.

As mentioned earlier, for the LPC TM model, trapped carbon particles are used to damage the tissue; however, they do not increase IOP alone and disappear 12 wk after Indian ink injection⁶⁹. These carbon particles form a cellular debris material that, when a laser is applied, creates a transient pseudomembrane on the trabecular spaces. As noted, the IOP decreases after laser treatments are stopped. However, the mechanism underlying this normalization of pressure is still elusive. One possible reason may be related to a decrease in cellular debris material and the occurrence of endothelial cell proliferation on the scarred TM tissue resulting in recovery of aqueous outflow⁸⁸. Studies have also reported that laser burn induces an increase in TM cell division, resulting in the upregulation of repair processes that could repopulate the TM and recover function^{89,90}. Additional work is warranted to better understand this phenomenon.

It should also be noted that TM methods are not suggested for albino rodents, as they do not have pigmented TM. However, several researchers have established an alternative rodent COH model by applying laser destruction at the post-trabecular level (discussed below; Table 2) which can be performed in albino rodents. Viral vector treatment may also be a better alternative for these animals. The elevation of IOP after viral vector injections seems to be dependent on method of injection, animal strain, and age. Unfortunately, injection of these vectors has been reported to cause ocular inflammation which may affect the outcome⁷⁵. These methods also need specialized equipment and training for handling, making them more expensive.

Table 2. Overview of Laser-induced COH Rodent Models.

Anatomical Position of Laser Treatment	Type of Laser	Animal	Duration (wk)	C_Mean IOP (mmHg)	G_Mean IOP (mmHg)	RGC Loss (%)	Axon Loss (%)	ERG	Remarks	References	
TM	Argon laser	WK rats	5	19.2 ± 0.9	22.0 ± 1.8		48.4		Injected Indian ink 1 wk prior to laser	69	
	Diode laser	Wistar rats	9	19.8 ± 1.6	25.5 ± 2.9		70.9		Laser power: 0.4 W, duration: 0.7 s	71	
	Diode laser	Wistar rats	9	19.5 ± 1.3	22.7 ± 3.4		49.7		Laser power: 0.4 W, duration: 0.7 s		
TM + episcleral veins	C57/BL6 mice	C57/BL6 mice	4	15.8 ± 0.8	27.4 ± 1.2				Laser power: 0.6 W, duration: 0.5 s	77	
			8	17.3 ± 0.7	19.5 ± 0.9				Injected indocyanine green into AC 20 min prior to laser treatment		
Limbus	Diode laser	BS mice	12	16.2 ± 2.4	20.1 ± 3.5				AC was flattened by aspirated AH	72	
			12	15.3 ± 2.0	19.4 ± 3.9		63.1		Loss of axons are proportion to the magnitude and duration of elevated IOP	73	
Limbal + episcleral veins	Diode laser	Wistar rats	9	19.3 ± 3.1	19.0 ± 4.2		4.6		Laser power: 1 W, duration: 0.2 s	71	
			8	16.0 ± 0.4	27.9 ± 0.6	33			Mean loss of 5.5% per week	78	
	Argon laser	Wistar rats	3	16	32	28		Memantine can significantly reduce the loss of RGCs compare to vehicle treated.	79		
Lewis rats		Lewis rats	3	15.8 ± 0.2	30.4 ± 0.42	0.28			Sustained IOP for at least 3 wk	80	
			5	11	23.6	29.8			2.4 times increased of NO production	81	
			4	14.9 ± 3.1	20.7 ± 2.6	21.7			12.6% loss of RGC at 2 wk time point	82	
	4	17.5 ± 3.70	26.75 ± 2.75				N1, P1 amplitude ↓; N/P ratio ↑	83			
		SD rats	SD rats	4	13.4 ± 0.7	22.1 ± 1.1	21.1			17% loss of RGC at 2 wk time point	84
				2	13.3 ± 0.7	24.5 ± 0.8	17.7			'betaB2-crystallin' was neuroprotective to RGCs	85
	C57BL/6j mice		C57BL/6j mice	4	11.2 ± 0.67	20.0 ± 2.8	27.3			Modified Schiotz-indentation tonometer were used to evaluate IOP	86
8				17.0 ± 2.2	20.0 ± 2.8	22.4			IOP raised in 90% treated eyes	87	

Abbreviations: COH, chronic ocular hypertension; IOP, intraocular pressure; C_Mean IOP, control eyes; G_Mean IOP, glaucoma eyes; mean IOP; G_Mean IOP, glaucoma eyes; mean IOP; G_Mean IOP, glaucoma eyes; mean IOP; Wistar Kyoto rats; BS mice, Black Swiss mice; SD rats, Sprague-Dawley rats; AC, anterior chamber; AH, aqueous humor; OP, oscillatory potentials; NO, nitric oxide; RGCs, retinal ganglion cells.

Post-TM Models

Another common area of the eye involved in balancing aqueous inflow and outflow that can be obstructed to increase IOP is the region posterior to the TM, particularly the episcleral veins. For post-trabecular COH models, a number of different methods have been developed and validated to impede the episcleral venous pathway.

Laser Treatments

While LPC is commonly used as a trabecular model of COH (as described above), WoldeMussie et al.⁷⁸ induced COH in rats by directly applying the argon laser to the limbal and episcleral vessels without interfering with the TM. In this model, LPC is performed on the veins approximately 0.5 to 0.8 mm away from the limbus as well as the episcleral drainage veins. After 2 consecutive laser treatments within a 1 wk interval, the IOP was observed to increase 2-fold compared to normal and remained at this level for 2 mo, resulting in a 44.2% loss of the RGCs. Further, the immunoreactivity of the intermediate filament glial fibrillary acidic protein (GFAP) was also increased in the Müller cells after 3 wk of induced hypertension. Various studies using this COH rodent model have also reported structural and functional changes similar to those observed in human glaucoma^{81–83}.

The effects of LPC on IOP were further evaluated by Levkovitch-Verbin et al.⁷¹. As described in the TM model section, in this study, a diode laser (532 nm) was used on various combinations of tissues, including the TM with the episcleral veins, the TM only, or the limbal and perilimbal veins only. With the exception of the limbal veins-only group, the elevated IOP was sustained for approximately 3 wk. A repeated laser treatment was also performed 1 wk after the first laser treatment for the eyes where the increase in IOP was less than 6 mmHg. In this experiment, the mean IOP after 6 wk for the combined group and TM group was 25.5 ± 2.9 mmHg and 22.0 ± 1.8 mmHg, respectively. Axonal loss was significantly increased with respect to the duration of increased IOP. In fact, in the combined group, the axonal loss was $16.1\% \pm 14.4\%$ after 1 wk ($P = 0.01$), $59.7\% \pm 25.7\%$ after 6 wk ($P < 0.001$), and $70.9\% \pm 23.6\%$ after 9 wk ($P < 0.001$). In contrast, the mean axonal loss for the TM-only group was $19.1\% \pm 14.0\%$ after 3 wk ($P = 0.004$), $24.3\% \pm 20.2\%$ after 6 wk ($P < 0.001$), and $48.4\% \pm 32.8\%$ after 9 wk ($P < 0.001$).

In order to increase the local photocoagulative effect of diode laser (810 nm) treatment, Grozdanic et al.⁷⁷ injected 10 μ L of photosensitive dye (10 mg/mL indocyanine green) into the AC of C57/BL6 mice 20 min prior to laser exposure and induction of COH. A significant, sustained increase in IOP was detected in the first 6 wk in 88% of the laser-treated eyes, which subsequently returned to normal levels after 8 wk. Notably, this study also detected a significant loss of RGCs, thinning of the retina, and degeneration of the optic nerve 8 wk after LPC, all of which appear to be associated

with a notable decrease in retinal function (i.e., the electroretinogram [ERG] responses). It is important to mention that these authors also administered topical pilocarpine 20 min prior to laser treatment to induce pupil miosis, which serves to protect the posterior pigmented structures of the eye from the diode laser energy during application of the laser to the TM and limbal veins.

To overcome the need for indocyanine green injection, Gross et al.⁸⁷ utilized an argon laser to damage the episcleral and limbal veins all around the eye to induce COH in mice, similar to a previous study using rats⁷⁸. This mouse model does not require corneal perforation and successfully elevated the IOP by 1.5-fold in 90% of the treated eyes, resulting in the loss of 23% of the RGCs by 4 wk compared to the untreated eyes. Similarly, Ji et al.⁸⁶ induced COH in mice by LPC of the limbal and episcleral veins. In doing so, they demonstrated that a single intervention of laser treatment can increase IOP by 7 mmHg, from a baseline of 13.0 ± 1.8 mmHg to 20.0 ± 2.8 mmHg. This increase sustained for 8 wk (17.0 ± 2.2 mmHg) and was associated with a 27% loss of RGCs after 4 wk⁸⁶.

Cauterization/Ligation of Episcleral Veins

Models utilizing cauterization. One of the earliest rat COH models for glaucoma research was the cauterization model, which was first demonstrated by Shareef et al.⁹¹, hence being designated the Shareef–Sharma model. This model involves cauterizing the episcleral veins (1 or multiple veins) in anesthetized rats with an ophthalmic cautery followed by exposure of the veins via incisions in the conjunctiva. Importantly, when using this method, care must be taken to minimize the damage to the surrounding conjunctiva and underlying sclera. When performed properly, this method produces a significant increase in IOP that is correlated with the number of cauterized veins. In fact, while single vein cauterization does not appear to significantly affect IOP, researchers observed a 1.5-fold elevation in IOP when 2 veins were cauterized that was maintained for at least 1.5 mo postsurgery. An IOP elevation of 1.9-fold for 2.5 mo was observed following the cauterization of 3 veins. The highest elevation (4.5-fold) was shown to occur after 1.5 wk in rats with 4 cauterized veins; however, cauterizing this number of veins also caused profound ocular complications, including proptosis, corneal edema, exposure keratopathy, and cataract, which were not observed in rats with fewer veins cauterized⁹¹. Histological analysis also showed that the level of RGC death in these rats was directly proportional to the increase in IOP as well as the duration of this increase⁹². Similarly, Sawada and Neufeld⁹³ showed an increase in IOP (1.6-fold) over a 6-mo period following cauterization of 3 veins. This increase was shown to cause cupping of the optic nerve head associated with a 40% loss of RGCs in the peripheral retina. Interestingly, the loss of RGCs per week was estimated to be 1.4% in the peripheral retina, but only 0.3% in the central retina, indicating that glaucoma-related vision

loss may be primarily due to the loss of cell function in the peripheral regions of this tissue.

A previous study by Mittag et al.⁹⁴ reported that cauterization of 3 veins resulted in an increase in IOP that lasted for 15 d, while repeated (4 to 5 times) injection of 5-fluorouracil, an antimetabolic agent that disrupts angiogenesis, in 3 to 4 d intervals after vein cauterization sustained this elevated IOP for at least 12 wk. This observation suggests that the growth of new vessels may result in increased episcleral venous patency. An electrophysiology study also showed that this technique can damage the photoreceptor cells as well as the bipolar cells, as the amplitude of both the a-wave and b-wave in their ERG analysis was significantly reduced in treated eyes compared to controls⁹⁵. The above findings suggest that the damage to the outer retinal layer may be due to ischemia in the tissue, which may limit the ability of this model to mimic human glaucoma^{94,95}.

While many cauterization models have used rats as a model, a mouse model has also been established. While cauterizing the episcleral veins in mice is more difficult because of their small size, Ruiz-Ederra and Verkman⁹⁶ were able to induce COH in albino cluster of differentiation 1 (CD1) mice. In fact, IOP was elevated in 87% of the treated eyes for 4 wk and was associated with a 20% loss of RGCs following a second round of cauterization (2 wk after the first treatment). However, in this study, one-third of the operated eyes were excluded due to surgery-related complications, such as vein leakage as well as conjunctiva and scleral tissue damage. In mice, it also appears that cauterization of 2 veins had no significant prolonged effect on the IOP, meaning that 3 or more veins would need to be operated on, which increases the chance of ocular damage and complications⁹⁶.

Models utilizing ligation. Ligation, similar in some ways to cauterization, is performed by suturing the episcleral veins to block the venous outflow. Notably, ligation of 3 episcleral veins has been shown to induce COH in adult rabbits. More recently, Yu et al.⁹⁷ demonstrated COH in female Wistar rats following ligation of 3 episcleral veins unilaterally with a 10/0 nylon suture after dissecting the overlying conjunctiva and Tenon's capsule. This method produced a sustained increase in IOP (24.5 ± 2.3 mmHg in operated eyes compared to 19.7 ± 1.9 mmHg in control eyes) for 7 mo in 40% of the treated eyes. This prolonged elevation of IOP caused optic disc cupping and a 35% loss of RGCs in 8 mo following the ligation. Although this method is relatively inexpensive, it requires excellent microsurgical skills in order to perform the ligation on the miniscule episcleral veins and treated eyes often (59.2%) require religation to elevate the IOP.

Ligation methods have also been established to induce COH in mice. For example, ligation of 3 to 5 veins over a 300° area using 11-0 nylon sutures was shown to cause COH in C57B1/6J mice⁹⁸. This method produced a sustained elevation in IOP (approximately 19 mmHg) for 10 wk compared to unoperated eyes (approximately 11 mmHg) and

caused a 30% decrease in viable RGCs. Notably, repeated surgeries at 1 wk intervals were needed for the eyes that did not have a measurable elevation in IOP initially.

Intraepiscleral Vein Injection with Hypertonic Saline

Another well-established posttrabecular obstruction method is the Moore–Morrison model⁹⁹, whereby COH is induced in a rat via cannulation of an aqueous vein with a 50- μ m glass microneedle followed by injection of a concentrated saline solution (2 M). Injection of this hypertonic solution was demonstrated to cause optic disc cupping, selective loss of RGCs, disorganization of the nerve fibers at the level of the lamina cribrosa, and loss of optic nerve axons. Furthermore, injection of saline into one of the radial episcleral veins also appears to cause sclerosis of the TM, which impedes AH outflow and raises IOP. This method involves placement of a polypropylene ring (C shaped) around the equator of the eye in the anesthetized rat which temporarily occludes or creates pressure in all of the episcleral veins except the one to which hypertonic saline is injected. The plastic ring is removed following injection of 50 μ L of sodium chloride (approximately 1.75 M) into the vein. This procedure drives the hypertonic saline from the site of injection into the TM and AC through Schlemm's canal after being injected into the exposed vein using a borosilicate glass microneedle. As a result, the IOP was shown to increase in the first 7 to 10 d and sustained for an extended period (200 d)¹⁰⁰. This increase occurred in approximately 60% of treated eyes and ranged from 10 to 35 mmHg above baseline levels^{99,101}. Notably, the variability in IOP elevation likely reflects the variability in the extent of sclerosis of the TM tissues following the saline injection. In fact, a second injection into another vein 180° away from the first vein was often needed in order to successfully induce elevation of the IOP. However, once an increase in IOP was observed, structural and functional changes in the retina were also detected, including RGC loss (39% to 93%), axon loss, extracellular matrix protein deposition at the optic nerve head, and progressive excavation of the optic disc, similar to other COH models. Fortune et al.¹⁰² also reported a 50% reduction in the positive scotopic threshold response (pSTR) after 5 wk of induced COH among Brown-Norway rats using this model. Interestingly, the functional and structural changes in this model appear to be significantly correlated with the extent of elevated IOP, but not with the duration of this increase¹⁰³. A recent study also reported an upregulation of inflammatory response signals and reorientation of the astrocytes in the optic nerve head in response to the elevated IOP¹⁰⁴. Alternatively, Morrison et al.¹⁰⁵ focused primarily on the effect of hypertonic saline concentration (from 1.6 to 2.0 M) on IOP. In doing so, they revealed that the higher concentration (>2.0 M) caused more destruction in the TM along with a higher increase in IOP that lasted for several months. However, injection of these higher concentrations of saline also appears to cause excessive inflammation and ciliary body

damage. Hence, a concentration of 1.74 M has become the standard for use in most rodent COH models of this variety.

Similar to the rat hypertonic saline-injected COH model, McKinnon et al.¹⁰⁶ also induced COH in C57BL/6 mice by injecting hypertonic saline (2.0 M) into an episcleral vein, which resulted in a 20% decrease in viable RGCs. In another study, 1.5 M saline was injected into C57BL/6 mouse eyes and produced a sustained increase in IOP (10.0 ± 3.3 mmHg) for at least 6 wk compared to controls (7.4 ± 2.2 mmHg)¹⁰⁷. However, in this study, 80% of the eyes required repeated injection during the 2nd and 4th wk to sustain the elevated IOP.

Circumlimbal Suture

Recently, a less invasive COH rat model was reported by Liu et al.¹⁰⁸, whereby an increase in IOP was induced in Long-Evans rats using a circumlimbal suturing technique. Here, 8/0 nylon suture was tied around the equator (approximately 1.5 mm behind the limbus) of the eye with 5 to 6 subconjunctival anchor points. Care was taken to avoid damage and direct pressure over the episcleral veins. This method produced a 7 to 10 mmHg increase in IOP compared to the baseline that lasted for 15 wk, resulting in progressive thinning of the nerve fiber layer (approximately 40%). ERG analysis also revealed a significant reduction in the amplitude of the a-wave (10.8%), b-wave (9.0%), and pSTR (26.7%) responses in the COH group. However, the reduction in photoreceptors and bipolar cells appeared to be stable for 2 wk after suturing, whereas the response of the RGCs (i.e., pSTR) progressively deteriorated from the 2nd to the 15th wk. Importantly, the suture material itself (untied) did not affect the IOP, structural morphology of the retina, or the ERG responses.

Technically, this method is relatively inexpensive and temporary, as the induced COH can be reversed simply by removing the suture. Furthermore, this method has less associated risk in terms of the chances of infection, as it is less invasive and only requires a single surgery. These attributes make this model useful for evaluating the efficacy of drugs aimed at reducing IOP as well as studies investigating neuroprotection for a longer time period. However, the extent of the initial spike in IOP and the exact mechanism underlying this increase in this model still remain unclear and further investigation is necessary.

General Points Concerning Post-TM Models

The post-TM models mentioned here are the most commonly used to induce COH in rodents. However, direct comparison between these methods is difficult as the techniques used for each are diverse, resulting in different levels and duration of IOP elevation. Therefore, variability in the structural and functional losses correlated to IOP elevation among these methods can be expected. Although they have their differences, each of these post-trabecular obstruction

methods is relatively inexpensive but requires surgical expertise in order to block the outflow drainage. They have been used extensively for evaluating the effect of elevated IOP, pathophysiology of glaucoma, and the neuroprotective effects of new drugs. However, these methods also have several limitations. For example, all post-trabecular methods directly or indirectly cause a certain extent of retinal and/or choroidal ischemia by blocking venous drainage. Therefore, these models may not be suitable when evaluating the efficacy of a drug which enhances the AH outflow facility to reduce IOP. In addition, angiogenesis-related mechanisms appear to be upregulated in the ocular vessels, which subsequently promote neovascularization and may also alter the pathophysiology of glaucoma by activating downstream protective mechanisms in the retinal neurons.

Topical Application of Corticosteroids

Induced ocular hypertension is a well-known consequence of steroid use among primates and nonprimate mammals, being first reported by McLean et al.¹⁰⁹ and Gordon et al.¹¹⁰. The mechanism underlying this phenomenon was later described by Francois and Victoria-Troncoso¹¹¹, whereby they suggest that steroids inhibit the activity of hyaluronidase, resulting in the accumulation of mucopolysaccharides within the TM, restricted aqueous outflow, and a subsequent increase in IOP. These changes are thought to mimic the etiology of primary open angle glaucoma in humans¹¹². More recently, similar steroid-induced changes in IOP have been documented in Wistar rats following the application of a topical steroid (dexamethasone) 4 times per day for 4 wk. In this study, a significant increase in IOP was noted after only 2 wk of steroid application compared to the controls¹¹³. Topical application of dexamethasone phosphate (0.1%) 3 times per day also caused a significant increase in IOP (7.7 ± 0.8 mmHg higher than control) in mouse eyes. This treatment resulted in a 55% reduction in the amplitude of the pattern ERG and a 16% decrease in viable RGCs after 20 wk of treatment compared to the controls¹¹⁴.

Although this model is inexpensive and technically easy to perform, the administration of steroids may introduce other functional changes as steroid treatment has been shown to facilitate neuroprotection as well as depression^{115,116}.

Comparison of Induced COH with Other Models

Transgenic Models

There are currently several transgenic rodent glaucoma models that have been developed and utilized to induce reproducible COH, including DBA/2J mice¹¹⁷, Col1a1^{r/r} mice¹¹⁸, Tyr423His Myoc mice¹¹⁹, Glutamate/aspartate-deficient mice¹²⁰, and Tg-MYCO^{Y437H} mice¹²¹. However, these models have several limitations when compared with the more common inducible COH rodent models. For example,

Table 3. Overview of Various Methods to Induce COH.

Level of Intervention	Procedure	Species	Specialized Material/ Instruments	Expertise	Expense*	References	
Invasive	Pre-trabecular	HA injection	Rat/mice	Hyaluronic acid	Micro surgery	+	50,51,125
		Microbeads	Rat/mice	Microbeads		+	53–55,60–65
		Magnetic microbeads	Rat/mice	Magnetic beads, magnet		+	57–59
	Trabecular	Viral vectors injection	Rat/mice	Viral vectors	Micro surgery	++	74–76
		Laser on TM	Rat/mice	Laser machine	Laser operation	++	69,70,72,73
	Post-trabecular	Laser on limbal and episcleral veins	Rat/mice	Laser machine	Laser operation	++	71,78,81–83,86,87,80,84,85
		Cauterization of episcleral veins	Rat/mice	Cautery	Micro surgery	+	91–96,126–129
		ligation of episcleral veins	Rat/mice	10-0/11-0 nylon suture		+	97,98
		Hypertonic saline injection into episcleral veins	Rat/mice	Customized plastic ring		+	100–105,130
		Circumlimbal suture	Rat/mice	8-0 nylon suture		+	108
Combination of Trabecular and post-trabecular	Laser on TM + Episcleral veins	Rat/mice	Laser machine	Laser operation	++	71,77	
	Topical corticosteroid	Rat/mice	Steroid drops	NA	NA	113,114,131–133	
Noninvasive							

Abbreviations: COH, chronic ocular hypertension; TM, trabecular meshwork; NA, not applicable; +, relatively mild expensive; ++, relatively moderate to high expensive.

*Relative expense.

transgenic rodents often only have mild to moderately elevated IOP levels with anterior segment anomalies. This is particularly true for the *Colla1^{tr}* mice, which have significantly higher IOP compared with the control mice at 18 (21% higher), 24 (44% higher), and 36 wk (36% higher) that is associated with AC abnormalities that may affect the final experimental outcome¹¹⁸. Furthermore, the time duration needed for rodents to manifest a glaucoma phenotype (6 to 18 mo) is longer than that needed for the inducible models, making these experiments more expensive, time-consuming, and labor-intensive¹⁸. These transgenic rodents also develop bilateral changes in IOP, thus another set of animals are required for use as the experimental controls.

Acute Optic Nerve Trauma

The acute optic nerve trauma models currently used to induce RGC death in rodents include various optic nerve crush models as well as full thickness or partial axotomy models^{122–124}. Notably, these models are known to cause apoptosis of all of the RGCs, with most of the cells dying within the first 2 wk following the initial trauma. However, these acute changes may or may not mimic those observed during chronic diseases when the patient is exposed to an insult for a relatively long period of time. Furthermore, during human glaucoma, RGC death and optic nerve changes are typically gradual. Thus, it is likely that the inducible COH models described earlier can be used to mimic human

glaucoma more effectively than these acute optic nerve trauma models.

Conclusions

Animal models of COH are useful tools for studying the etiology of human glaucoma during disease onset and pathological progression as well as the effect of therapies in a controlled and reproducible manner. These models have been extensively used to enhance our understanding of the IOP-related changes observed in the eyes of glaucoma patients and have clearly demonstrated the involvement of COH in the morphological and functional damage that occurs in their retinas. Importantly, when choosing the ideal COH rodent model for a glaucoma study, researchers should be aware of the various advantages and disadvantages of each. Some general characteristics that should be preferred are that the model is minimally invasive, inexpensive, and easy to perform. Moreover, the model should be able to produce a sustained elevation in IOP for a prolonged period (>6 wk) that results in RGC death and loss of function without interfering with the photoreceptors or other neurons in the retina. Finally, no surgically induced complications, such as intraocular bleeding, analysis obstruction (e.g., retinal imaging), or damage to the optic nerve head, should occur. Unfortunately, no single COH model currently in use incorporates all of these features.

While the present review is the first to compare these specific methods (Table 3), others have previously

highlighted the similarities and differences among different glaucoma models^{134–137}. McKinnon et al.¹³⁸, for instance, compared the hypertonic saline injection model, cautery models, and limbal laser (argon) model. In their analysis, the laser-induced model appeared to produce the most reproducible sustained elevation of IOP (occurring in 100% of the animals compared to 42% and 49% for the hypertonic saline and cautery models, respectively) but also appeared to cause optic nerve damage in 83% while only 36% and 20% were damaged for the other models. Similarly, Urcola et al.⁵³ previously compared the cautery, injected microsphere, and injected microsphere with HPM models, which produced RGC death in $28.5\% \pm 2.4\%$, $23.1\% \pm 2.1\%$, and $27.2\% \pm 2.1\%$ of the animals, respectively. These other reviews, much like the current analysis, largely recommend weighing the advantages and disadvantages of each model before designing the study. Unlike previous analyses, however, we have provided a more thorough evaluation of these models based on the ocular tissue targeted (pre-trabecular, trabecular, or post-trabecular). Furthermore, this review is particularly relevant for researchers interested in using these rodent models to investigate the use of various therapies, such as cell transplantation. In fact, multiple cell transplantation studies using a variety of cell types, including mesenchymal stromal cells^{17,21,22} and pluripotent stem cells^{18,139}, have indicated that this technique may mediate neuroprotection of the RGCs and help restore IOP regulatory mechanisms during glaucoma^{18,139}. Utilizing 1 or more of the rodent models described here will further elucidate the possible therapeutic applications of these treatments.

The future of glaucoma research will be fundamentally based on the continual development of suitable COH models. These models are essential to advancing our understanding of the physiological mechanisms functioning during glaucoma onset and pathogenesis as well as for analyzing novel glaucoma therapies. Additionally, there have also been numerous advances in the technology used to assess glaucomatous damage, including the measurement of IOP, RGC death, optic nerve damage, and retinal function. Utilization of these new technologies in basic science and biotechnology studies will continue to lead to the development of better translational glaucoma models and the subsequent enrichment of patient treatment and care.

Declaration of Conflicting Interests

The author(s) declared no potential conflicts of interest with respect to the research, authorship, and/or publication of this article.

Funding

The author(s) disclosed receipt of the following financial support for the research and/or authorship of this article: This work is supported by RGC GRF PolyU 5607/12M and PolyU internal funds G-UB83 and G-UAAE (to C-W. D.) as well as Seed funding programmer for Basic Research, The University of Hong Kong 201511159295 (to K.C.).

References

1. Quigley HA, Broman AT. The number of people with glaucoma worldwide in 2010 and 2020. *Br J Ophthalmol*. 2006; 90(3):262–267.
2. Leske MC. The epidemiology of open-angle glaucoma: a review. *Am J Epidemiol*. 1983;118(2):166–191.
3. Kass MA, Heuer DK, Higginbotham EJ, Johnson CA, Keltner JL, Miller JP, Parrish RK II, Wilson MR, Gordon MO. The Ocular Hypertension Treatment Study: a randomized trial determines that topical ocular hypotensive medication delays or prevents the onset of primary open-angle glaucoma. *Arch Ophthalmol*. 2002;120(6):701–713; discussion 829–830.
4. Gordon MO, Beiser JA, Brandt JD, Heuer DK, Higginbotham EJ, Johnson CA, Keltner JL, Miller JP, Parrish RK II, Wilson MR, Kass MA. The Ocular Hypertension Treatment Study: baseline factors that predict the onset of primary open-angle glaucoma. *Arch Ophthalmol*. 2002;120(6):714–720; discussion 829–830.
5. Le A, Mukesh BN, McCarty CA, Taylor HR. Risk factors associated with the incidence of open-angle glaucoma: the visual impairment project. *Invest Ophthalmol Vis Sci*. 2003; 44(9):3783–3789.
6. Heijl A, Leske MC, Bengtsson B, Hyman L, Bengtsson B, Hussein M. Reduction of intraocular pressure and glaucoma progression: results from the early manifest glaucoma trial. *Arch Ophthalmol*. 2002;120(10):1268–1279.
7. Drance S, Anderson DR, Schulzer M; Collaborative Normal-Tension Glaucoma Study Group. Risk factors for progression of visual field abnormalities in normal-tension glaucoma. *Am J Ophthalmol*. 2001;131(6):699–708.
8. Davis BM, Crawley L, Pahlitzsch M, Javaid F, Cordeiro MF. Glaucoma: the retina and beyond. *Acta Neuropathol*. 2016; 132(6):807–826.
9. Kaushik S, Pandav SS, Ram J. Neuroprotection in glaucoma. *J Postgrad Med*. 2003;49(1):90–95.
10. Danesh-Meyer HV. Neuroprotection in glaucoma: recent and future directions. *Curr Opin Ophthalmol*. 2011;22(2):78–86.
11. Almasieh M, Wilson AM, Morquette B, Cueva Vargas JL, Di Polo A. The molecular basis of retinal ganglion cell death in glaucoma. *Prog Retin Eye Res*. 2012;31(2):152–181.
12. Kuehn MH, Fingert JH, Kwon YH. Retinal ganglion cell death in glaucoma: mechanisms and neuroprotective strategies. *Ophthalmol Clin North Am*. 2005;18(3):383–395, vi.
13. Osborne NN, Melena J, Chidlow G, Wood JP. A hypothesis to explain ganglion cell death caused by vascular insults at the optic nerve head: possible implication for the treatment of glaucoma. *Br J Ophthalmol*. 2001;85(10):1252–1259.
14. Johnson TV, Martin KR. Cell transplantation approaches to retinal ganglion cell neuroprotection in glaucoma. *Curr Opin Pharmacol*. 2013;13(1):78–82.
15. Zarbin M. Cell-based therapy for degenerative retinal disease. *Trends Mol Med*. 2016;22(2):115–134.
16. Sun Y, Williams A, Waisbourd M, Iacovitti L, Katz LJ. Stem cell therapy for glaucoma: science or snake oil? *Surv Ophthalmol*. 2015;60(2):93–105.

17. Roubeix C, Godefroy D, Mias C, Sapienza A, Riancho L, Degardin J, Fradot V, Ivkovic I, Picaud S, Sennlaub F, Denoyer A, Rostene W, Sahel JA, Parsadaniantz SM, Brignole-Baudouin F, Baudouin C. Intraocular pressure reduction and neuroprotection conferred by bone marrow-derived mesenchymal stem cells in an animal model of glaucoma. *Stem Cell Res Ther.* 2015;6:177.
18. Zhu W, Gramlich OW, Laboissonniere L, Jain A, Sheffield VC, Trimarchi JM, Tucker BA, Kuehn MH. Transplantation of iPSC-derived TM cells rescues glaucoma phenotypes in vivo. *Proc Natl Acad Sci U S A.* 2016;113(25):E3492–E3500.
19. Johnson TV, Bull ND, Hunt DP, Marina N, Tomarev SI, Martin KR. Neuroprotective effects of intravitreal mesenchymal stem cell transplantation in experimental glaucoma. *Invest Ophthalmol Vis Sci.* 2010;51(4):2051–2059.
20. Harper MM, Grozdanic SD, Blits B, Kuehn MH, Zamzow D, Buss JE, Kardon RH, Sakaguchi DS. Transplantation of BDNF-secreting mesenchymal stem cells provides neuroprotection in chronically hypertensive rat eyes. *Invest Ophthalmol Vis Sci.* 2011;52(7):4506–4515.
21. Emre E, Yuksel N, Duruksu G, Pirhan D, Subasi C, Erman G, Karaoz E. Neuroprotective effects of intravitreally transplanted adipose tissue and bone marrow-derived mesenchymal stem cells in an experimental ocular hypertension model. *Cytotherapy.* 2015;17(5):543–559.
22. Mead B, Hill LJ, Blanch RJ, Ward K, Logan A, Berry M, Leadbeater W, Scheven BA. Mesenchymal stromal cell-mediated neuroprotection and functional preservation of retinal ganglion cells in a rodent model of glaucoma. *Cytotherapy.* 2016;18(4):487–496.
23. Mead B, Logan A, Berry M, Leadbeater W, Scheven BA. Intravitreally transplanted dental pulp stem cells promote neuroprotection and axon regeneration of retinal ganglion cells after optic nerve injury. *Invest Ophthalmol Vis Sci.* 2013;54(12):7544–7556.
24. Zhang R, Zhang H, Xu L, Ma K, Wallrapp C, Jonas JB. Neuroprotective effect of intravitreal cell-based glucagon-like peptide-1 production in the optic nerve crush model. *Acta Ophthalmol.* 2011;89(4):e320–e326.
25. Bouhenni RA, Dumire J, Sewell A, Edward DP. Animal models of glaucoma. *J Biomed Biotechnol.* 2012;2012:692609.
26. Tomarev S. Animal models of glaucoma. *Encyclopedia of the Eye.* 2010:106–111.
27. Weinreb RN, Lindsey JD. The importance of models in glaucoma research. *J Glaucoma.* 2005;14(4):302–324.
28. Albrecht May C. Comparative anatomy of the optic nerve head and inner retina in non-primate animal models used for glaucoma research. *Open Ophthalmol J.* 2008;2:94–101.
29. Morrison J, Farrell S, Johnson E, Deppmeier L, Moore CG, Grossmann E. Structure and composition of the rodent lamina cribrosa. *Exp Eye Res.* 1995;60(2):127–135.
30. Chen L, Zhao Y, Zhang H. Comparative anatomy of the trabecular meshwork, the optic nerve head and the inner retina in rodent and primate models used for glaucoma research. *Vision.* 2016;1(1):4.
31. van der Zypen E. Experimental morphological study on structure and function of the filtration angle of the rat eye. *Ophthalmologica.* 1977;174(5):285–298.
32. Morrison JC, Fraunfelder FW, Milne ST, Moore CG. Limbal microvasculature of the rat eye. *Invest Ophthalmol Vis Sci.* 1995;36(3):751–756.
33. Morcos Y, Chan-Ling T. Concentration of astrocytic filaments at the retinal optic nerve junction is coincident with the absence of intra-retinal myelination: comparative and developmental evidence. *J Neurocytol.* 2000;29(9):665–678.
34. Smith RS, Zabaleta A, Savinova OV, John SW. The mouse anterior chamber angle and trabecular meshwork develop without cell death. *BMC Dev Biol.* 2001;1:3.
35. May CA, Lutjen-Drecoll E. Morphology of the murine optic nerve. *Invest Ophthalmol Vis Sci.* 2002;43(7):2206–2212.
36. Aihara M, Lindsey JD, Weinreb RN. Aqueous humor dynamics in mice. *Invest Ophthalmol Vis Sci.* 2003;44(12):5168–5173.
37. Johnson TV, Tomarev SI. Rodent models of glaucoma. *Brain Res Bull.* 2010;81(2–3):349–358.
38. Dismuke WM, Overby DR, Civan MM, Stamer WD. The value of mouse models for glaucoma drug discovery. *J Ocul Pharmacol Ther.* 2016;32(8):486–487.
39. Vecino E, Sharma SC. Glaucoma animal models. *European Union: INTECH Open Access Publisher;* 2011;319–334.
40. Fraser JR, Laurent TC, Laurent UB. Hyaluronan: its nature, distribution, functions and turnover. *J Intern Med.* 1997;242(1):27–33.
41. Lerner LE, Polansky JR, Howes EL, Stern R. Hyaluronan in the human trabecular meshwork. *Invest Ophthalmol Vis Sci.* 1997;38(6):1222–1228.
42. Toole BP. Hyaluronan in morphogenesis. *J Intern Med.* 1997;242(1):35–40.
43. Knepper PA, Goossens W, Hvizd M, Palmberg PF. Glycosaminoglycans of the human trabecular meshwork in primary open-angle glaucoma. *Invest Ophthalmol Vis Sci.* 1996;37(7):1360–1367.
44. Navajas EV, Martins JR, Melo LA, Jr., Saraiva VS, Dietrich CP, Nader HB, Belfort R Jr. Concentration of hyaluronic acid in primary open-angle glaucoma aqueous humor. *Exp Eye Res.* 2005;80(6):853–857.
45. Gartaganis SP, Georgakopoulos CD, Exarchou AM, Mela EK, Lamari F, Karamanos NK. Increased aqueous humor basic fibroblast growth factor and hyaluronan levels in relation to the exfoliation syndrome and exfoliation glaucoma. *Acta Ophthalmol Scand.* 2001;79(6):572–575.
46. Goa KL, Benfield P. Hyaluronic acid. A review of its pharmacology and use as a surgical aid in ophthalmology, and its therapeutic potential in joint disease and wound healing. *Drugs.* 1994;47(3):536–566.
47. Barron BA, Busin M, Page C, Bergsma DR, Kaufman HE. Comparison of the effects of Viscoat and Healon on postoperative intraocular pressure. *Am J Ophthalmol.* 1985;100(3):377–384.
48. Mac Rae SM, Edelhauser HF, Hyndiuk RA, Burd EM, Schultz RO. The effects of sodium hyaluronate, chondroitin sulfate,

- and methylcellulose on the corneal endothelium and intraocular pressure. *Am J Ophthalmol.* 1983;95(3):332–341.
49. Henry JC, Olander K. Comparison of the effect of four viscoelastic agents on early postoperative intraocular pressure. *J Cataract Refract Surg.* 1996;22(7):960–966.
 50. Benozzi J, Nahum LP, Campanelli JL, Rosenstein RE. Effect of hyaluronic acid on intraocular pressure in rats. *Invest Ophthalmol Vis Sci.* 2002;43(7):2196–2200.
 51. Moreno MC, Marcos HJ, Oscar Croxatto J, Sande PH, Campanelli J, Jaliffa CO, Benozzi J, Rosenstein RE. A new experimental model of glaucoma in rats through intracameral injections of hyaluronic acid. *Exp Eye Res.* 2005;81(1):71–80.
 52. Weber AJ, Zelenak D. Experimental glaucoma in the primate induced by latex microspheres. *J Neurosci Methods.* 2001;111(1):39–48.
 53. Urcola JH, Hernandez M, Vecino E. Three experimental glaucoma models in rats: comparison of the effects of intraocular pressure elevation on retinal ganglion cell size and death. *Exp Eye Res.* 2006;83(2):429–437.
 54. Sappington RM, Carlson BJ, Crish SD, Calkins DJ. The microbead occlusion model: a paradigm for induced ocular hypertension in rats and mice. *Invest Ophthalmol Vis Sci.* 2010;51(1):207–216.
 55. Cone-Kimball E, Nguyen C, Oglesby EN, Pease ME, Steinhart MR, Quigley HA. Scleral structural alterations associated with chronic experimental intraocular pressure elevation in mice. *Mol Vis.* 2013;19:2023–2039.
 56. McBain SC, Yiu HH, Dobson J. Magnetic nanoparticles for gene and drug delivery. *Int J Nanomedicine.* 2008;3(2):169–180.
 57. Samsel PA, Kisiswa L, Erichsen JT, Cross SD, Morgan JE. A novel method for the induction of experimental glaucoma using magnetic microspheres. *Invest Ophthalmol Vis Sci.* 2011;52(3):1671–1675.
 58. Dai C, Khaw PT, Yin ZQ, Li D, Raisman G, Li Y. Structural basis of glaucoma: the fortified astrocytes of the optic nerve head are the target of raised intraocular pressure. *Glia.* 2012;60(1):13–28.
 59. Bunker S, Holeniewska J, Vijay S, Dahlmann-Noor A, Khaw P, Ng YS, Shima D, Foxton R. Experimental glaucoma induced by ocular injection of magnetic microspheres. *J Vis Exp.* 2015;96:5.
 60. Cone FE, Gelman SE, Son JL, Pease ME, Quigley HA. Differential susceptibility to experimental glaucoma among 3 mouse strains using bead and viscoelastic injection. *Exp Eye Res.* 2010;91(3):415–424.
 61. Kalesnykas G, Oglesby EN, Zack DJ, Cone FE, Steinhart MR, Tian J, Pease ME, Quigley HA. Retinal ganglion cell morphology after optic nerve crush and experimental glaucoma. *Invest Ophthalmol Vis Sci.* 2012;53(7):3847–3857.
 62. Cone FE, Steinhart MR, Oglesby EN, Kalesnykas G, Pease ME, Quigley HA. The effects of anesthesia, mouse strain and age on intraocular pressure and an improved murine model of experimental glaucoma. *Exp Eye Res.* 2012;99:27–35.
 63. Frankfort BJ, Khan AK, Tse DY, Chung I, Pang JJ, Yang Z, Gross RL, Wu SM. Elevated intraocular pressure causes inner retinal dysfunction before cell loss in a mouse model of experimental glaucoma. *Invest Ophthalmol Vis Sci.* 2013;54(1):762–770.
 64. Smedowski A, Pietrucha-Dutczak M, Kaarniranta K, Lewin-Kowalik J. A rat experimental model of glaucoma incorporating rapid-onset elevation of intraocular pressure. *Sci Rep.* 2014;4:5910.
 65. Khan AK, Tse DY, van der Heijden ME, Shah P, Nusbaum DM, Yang Z, Wu SM, Frankfort BJ. Prolonged elevation of intraocular pressure results in retinal ganglion cell loss and abnormal retinal function in mice. *Exp Eye Res.* 2015;130:29–37.
 66. Ho LC, Conner IP, Do CW, Kim SG, Wu EX, Wollstein G, Schuman JS, Chan KC. In vivo assessment of aqueous humor dynamics upon chronic ocular hypertension and hypotensive drug treatment using gadolinium-enhanced MRI. *Invest Ophthalmol Vis Sci.* 2014;55(6):3747–3757.
 67. Gaasterland D, Kupfer C. Experimental glaucoma in the rhesus monkey. *Invest Ophthalmol.* 1974;13(6):455–457.
 68. Krauss JM, Puliafito CA. Lasers in ophthalmology. *Lasers Surg Med.* 1995;17(2):102–159.
 69. Ueda J, Sawaguchi S, Hanyu T, Yaoeda K, Fukuchi T, Abe H, Ozawa H. Experimental glaucoma model in the rat induced by laser trabecular photocoagulation after an intracameral injection of India ink. *Jpn J Ophthalmol.* 1998;42(5):337–344.
 70. Park KH, Cozier F, Ong OC, Caprioli J. Induction of heat shock protein 72 protects retinal ganglion cells in a rat glaucoma model. *Invest Ophthalmol Vis Sci.* 2001;42(7):1522–1530.
 71. Levkovitch-Verbin H, Quigley HA, Martin KR, Valenta D, Baumrind LA, Pease ME. Translimbal laser photocoagulation to the trabecular meshwork as a model of glaucoma in rats. *Invest Ophthalmol Vis Sci.* 2002;43(2):402–410.
 72. Aihara M, Lindsey JD, Weinreb RN. Experimental mouse ocular hypertension: establishment of the model. *Invest Ophthalmol Vis Sci.* 2003;44(10):4314–4320.
 73. Mabuchi F, Aihara M, Mackey MR, Lindsey JD, Weinreb RN. Optic nerve damage in experimental mouse ocular hypertension. *Invest Ophthalmol Vis Sci.* 2003;44(10):4321–4330.
 74. Pang IH, Millar JC, Clark AF. Elevation of intraocular pressure in rodents using viral vectors targeting the trabecular meshwork. *Exp Eye Res.* 2015;141:33–41.
 75. Shepard AR, Millar JC, Pang IH, Jacobson N, Wang WH, Clark AF. Adenoviral gene transfer of active human transforming growth factor- β 2 elevates intraocular pressure and reduces outflow facility in rodent eyes. *Invest Ophthalmol Vis Sci.* 2010;51(4):2067–2076.
 76. Buie LK, Karim MZ, Smith MH, Borrás T. Development of a model of elevated intraocular pressure in rats by gene transfer of bone morphogenetic protein 2. *Invest Ophthalmol Vis Sci.* 2013;54(8):5441–5455.
 77. Grozdanic SD, Betts DM, Sakaguchi DS, Allbaugh RA, Kwon YH, Kardon RH. Laser-induced mouse model of chronic ocular hypertension. *Invest Ophthalmol Vis Sci.* 2003;44(10):4337–4346.

78. WoldeMussie E, Ruiz G, Wijono M, Wheeler LA. Neuroprotection of retinal ganglion cells by brimonidine in rats with laser-induced chronic ocular hypertension. *Invest Ophthalmol Vis Sci.* 2001;42(12):2849–2855.
79. Hare W, WoldeMussie E, Lai R, Ton H, Ruiz G, Feldmann B, Wijono M, Chun T, Wheeler L. Efficacy and safety of memantine, an NMDA-type open-channel blocker, for reduction of retinal injury associated with experimental glaucoma in rat and monkey. *Surv Ophthalmol.* 2001;45(suppl 3):S284–S289; discussion S295–S296.
80. Schori H, Kipnis J, Yoles E, WoldeMussie E, Ruiz G, Wheeler LA, Schwartz M. Vaccination for protection of retinal ganglion cells against death from glutamate cytotoxicity and ocular hypertension: implications for glaucoma. *Proc Natl Acad Sci U S A.* 2001;98(6):3398–3403.
81. Siu AW, Leung MC, To CH, Siu FK, Ji JZ, So KF. Total retinal nitric oxide production is increased in intraocular pressure-elevated rats. *Exp Eye Res.* 2002;75(4):401–406.
82. Ji JZ, Elyaman W, Yip HK, Lee VW, Yick LW, Hugon J, So KF. CNTF promotes survival of retinal ganglion cells after induction of ocular hypertension in rats: the possible involvement of STAT3 pathway. *Eur J Neurosci.* 2004;19(2):265–272.
83. Chan HH, Leung MC, So KF. Electroacupuncture provides a new approach to neuroprotection in rats with induced glaucoma. *J Altern Complement Med.* 2005;11(2):315–322.
84. Chan HC, Chang RC, Koon-Ching Ip A, Chiu K, Yuen WH, Zee SY, So KF. Neuroprotective effects of *Lycium barbarum* Lynn on protecting retinal ganglion cells in an ocular hypertension model of glaucoma. *Exp Neurol.* 2007;203(1):269–273.
85. Chiu K, Zhou Y, Yeung SC, Lok CK, Chan OO, Chang RC, So KF, Chiu JF. Up-regulation of crystallins is involved in the neuroprotective effect of wolfberry on survival of retinal ganglion cells in rat ocular hypertension model. *J Cell Biochem.* 2010;110(2):311–320.
86. Ji J, Chang P, Pennesi ME, Yang Z, Zhang J, Li D, Wu SM, Gross RL. Effects of elevated intraocular pressure on mouse retinal ganglion cells. *Vision Res.* 2005;45(2):169–179.
87. Gross RL, Ji J, Chang P, Pennesi ME, Yang Z, Zhang J, Wu SM. A mouse model of elevated intraocular pressure: retina and optic nerve findings. *Trans Am Ophthalmol Soc.* 2003;101:163–169; discussion 169–171.
88. Wang RF, Schumer RA, Serle JB, Podos SM. A comparison of argon laser and diode laser photocoagulation of the trabecular meshwork to produce the glaucoma monkey model. *J Glaucoma.* 1998;7(1):45–49.
89. Acott TS, Samples JR, Bradley JM, Bacon DR, Bylsma SS, Van Buskirk EM. Trabecular repopulation by anterior trabecular meshwork cells after laser trabeculoplasty. *Am J Ophthalmol.* 1989;107(1):1–6.
90. Dueker DK, Norberg M, Johnson DH, Tschumper RC, Feeney-Burns L. Stimulation of cell division by argon and Nd:YAG laser trabeculoplasty in cynomolgus monkeys. *Invest Ophthalmol Vis Sci.* 1990;31(1):115–124.
91. Shareef SR, Garcia-Valenzuela E, Salierno A, Walsh J, Sharma SC. Chronic ocular hypertension following episcleral venous occlusion in rats. *Exp Eye Res.* 1995;61(3):379–382.
92. Garcia-Valenzuela E, Shareef S, Walsh J, Sharma SC. Programmed cell death of retinal ganglion cells during experimental glaucoma. *Exp Eye Res.* 1995;61(1):33–44.
93. Sawada A, Neufeld AH. Confirmation of the rat model of chronic, moderately elevated intraocular pressure. *Exp Eye Res.* 1999;69(5):525–531.
94. Mittag TW, Danias J, Pohorenc G, Yuan HM, Burakgazi E, Chalmers-Redman R, Podos SM, Tatton WG. Retinal damage after 3 to 4 months of elevated intraocular pressure in a rat glaucoma model. *Invest Ophthalmol Vis Sci.* 2000;41(11):3451–3459.
95. Bayer AU, Danias J, Brodie S, Maag KP, Chen B, Shen F, Podos SM, Mittag TW. Electroretinographic abnormalities in a rat glaucoma model with chronic elevated intraocular pressure. *Exp Eye Res.* 2001;72(6):667–677.
96. Ruiz-Ederra J, Verkman AS. Mouse model of sustained elevation in intraocular pressure produced by episcleral vein occlusion. *Exp Eye Res.* 2006;82(5):879–884.
97. Yu S, Tanabe T, Yoshimura N. A rat model of glaucoma induced by episcleral vein ligation. *Exp Eye Res.* 2006;83(4):758–770.
98. Zhu Y, Zhang L, Schmidt JF, Gidday JM. Glaucoma-induced degeneration of retinal ganglion cells prevented by hypoxic preconditioning: a model of glaucoma tolerance. *Mol Med.* 2012;18:697–706.
99. Moore C, Milne S, Morrison J. A rat model of pressure-induced optic nerve damage. Philadelphia, PA: Lippincott-Raven; 1993:1141–1141.
100. Johnson EC, Morrison JC, Farrell S, Deppmeier L, Moore CG, McGinty MR. The effect of chronically elevated intraocular pressure on the rat optic nerve head extracellular matrix. *Exp Eye Res.* 1996;62(6):663–674.
101. Hanninen VA, Pantcheva MB, Freeman EE, Poulin NR, Groskreutz CL. Activation of caspase 9 in a rat model of experimental glaucoma. *Curr Eye Res.* 2002;25(6):389–395.
102. Fortune B, Bui BV, Morrison JC, Johnson EC, Dong J, Cepurna WO, Jia L, Barber S, Cioffi GA. Selective ganglion cell functional loss in rats with experimental glaucoma. *Invest Ophthalmol Vis Sci.* 2004;45(6):1854–1862.
103. Chauhan BC, Pan J, Archibald ML, LeVatte TL, Kelly ME, Tremblay F. Effect of intraocular pressure on optic disc topography, electroretinography, and axonal loss in a chronic pressure-induced rat model of optic nerve damage. *Invest Ophthalmol Vis Sci.* 2002;43(9):2969–2976.
104. Tehrani S, Johnson EC, Cepurna WO, Morrison JC. Astrocyte processes label for filamentous actin and reorient early within the optic nerve head in a rat glaucoma model. *Invest Ophthalmol Vis Sci.* 2014;55(10):6945–6952.
105. Morrison JC, Moore CG, Deppmeier LM, Gold BG, Meshul CK, Johnson EC. A rat model of chronic pressure-induced optic nerve damage. *Exp Eye Res.* 1997;64(1):85–96.
106. McKinnon S, Reitsamer H, Ransom N, Caldwell M, Harrison J, Kiel J. Induction and tonopen measurement of ocular hypertension in C57BL/6 mice. *Invest Ophthalmol Vis Sci.* 2003;44(13):3319–3319.

107. Kipfer-Kauer A, McKinnon SJ, Frueh BE, Goldblum D. Distribution of amyloid precursor protein and amyloid-beta in ocular hypertensive C57BL/6 mouse eyes. *Curr Eye Res.* 2010;35(9):828–834.
108. Liu HH, Bui BV, Nguyen CT, Kezic JM, Vingrys AJ, He Z. Chronic ocular hypertension induced by circumlimbal suture in rats. *Invest Ophthalmol Vis Sci.* 2015;56(5):2811–2820.
109. McLean J, Gordon DM, Koteen H. Clinical experiences with ACTH and cortisone in ocular diseases. *Trans Am Acad Ophthalmol Otolaryngol.* 1951;55:565–572.
110. Gordon DM, Mc LJ, Koteen H, Bousquet FP, Mc CW, Baras I, Wetzig P, Norton EW. The use of ACTH and cortisone in ophthalmology. *Am J Ophthalmol.* 1951;34(12):1675–1686.
111. Francois J, Victoria-Troncoso V. Corticosteroid glaucoma. *Ophthalmologica.* 1977;174(4):195–209.
112. Overby DR, Clark AF. Animal models of glucocorticoid-induced glaucoma. *Exp Eye Res.* 2015;141:15–22.
113. Sawaguchi K, Nakamura Y, Nakamura Y, Sakai H, Sawaguchi S. Myocilin gene expression in the trabecular meshwork of rats in a steroid-induced ocular hypertension model. *Ophthalmic Res.* 2005;37(5):235–242.
114. Zode GS, Sharma AB, Lin X, Searby CC, Bugge K, Kim GH, Clark AF, Sheffield VC. Ocular-specific ER stress reduction rescues glaucoma in murine glucocorticoid-induced glaucoma. *J Clin Invest.* 2014;124(5):1956–1965.
115. Patten SB, Neutel CI. Corticosteroid-induced adverse psychiatric effects: incidence, diagnosis and management. *Drug Saf.* 2000;22(2):111–122.
116. Po KT, Siu AM, Lau BW, Chan JN, So KF, Chan CC. Repeated, high-dose dextromethorphan treatment decreases neurogenesis and results in depression-like behavior in rats. *Exp Brain Res.* 2015;233(7):2205–2214.
117. Chang B, Smith RS, Hawes NL, Anderson MG, Zabaleta A, Savinova O, Roderick TH, Heckenlively JR, Davisson MT, John SW. Interacting loci cause severe iris atrophy and glaucoma in DBA/2J mice. *Nat Genet.* 1999;21(4):405–409.
118. Aihara M, Lindsey JD, Weinreb RN. Ocular hypertension in mice with a targeted type I collagen mutation. *Invest Ophthalmol Vis Sci.* 2003;44(4):1581–1585.
119. Senatorov V, Malyukova I, Fariss R, Wawrousek EF, Swaminathan S, Sharan SK, Tomarev S. Expression of mutated mouse myocilin induces open-angle glaucoma in transgenic mice. *J Neurosci.* 2006;26(46):11903–11914.
120. Harada C, Namekata K, Guo X, Yoshida H, Mitamura Y, Matsumoto Y, Tanaka K, Ichijo H, Harada T. ASK1 deficiency attenuates neural cell death in GLAST-deficient mice, a model of normal tension glaucoma. *Cell Death Differ.* 2010;17(11):1751–1759.
121. Zode GS, Kuehn MH, Nishimura DY, Searby CC, Mohan K, Grozdanic SD, Bugge K, Anderson MG, Clark AF, Stone EM, Sheffield VC. Reduction of ER stress via a chemical chaperone prevents disease phenotypes in a mouse model of primary open angle glaucoma. *J Clin Invest.* 2011;121(9):3542–3553.
122. Levkovitch-Verbin H, Harris-Cerruti C, Groner Y, Wheeler LA, Schwartz M, Yoles E. RGC death in mice after optic nerve crush injury: oxidative stress and neuroprotection. *Invest Ophthalmol Vis Sci.* 2000;41(13):4169–4174.
123. Villegas-Perez MP, Vidal-Sanz M, Rasminsky M, Bray GM, Aguayo AJ. Rapid and protracted phases of retinal ganglion cell loss follow axotomy in the optic nerve of adult rats. *J Neurobiol.* 1993;24(1):23–36.
124. Berkelaar M, Clarke DB, Wang YC, Bray GM, Aguayo AJ. Axotomy results in delayed death and apoptosis of retinal ganglion cells in adult rats. *J Neurosci.* 1994;14(7):4368–4374.
125. Mayordomo-Febrer A, Lopez-Murcia M, Morales-Tatay JM, Monleon-Salvado D, Pinazo-Duran MD. Metabolomics of the aqueous humor in the rat glaucoma model induced by a series of intracameral sodium hyaluronate injection. *Exp Eye Res.* 2015;131:84–92.
126. Ahmed FA, Hegazy K, Chaudhary P, Sharma SC. Neuroprotective effect of alpha(2) agonist (brimonidine) on adult rat retinal ganglion cells after increased intraocular pressure. *Brain Res.* 2001;913(2):133–139.
127. Ko ML, Hu DN, Ritch R, Sharma SC, Chen CF. Patterns of retinal ganglion cell survival after brain-derived neurotrophic factor administration in hypertensive eyes of rats. *Neurosci Lett.* 2001;305(2):139–142.
128. Naskar R, Wissing M, Thanos S. Detection of early neuron degeneration and accompanying microglial responses in the retina of a rat model of glaucoma. *Invest Ophthalmol Vis Sci.* 2002;43(9):2962–2968.
129. Neufeld AH, Sawada A, Becker B. Inhibition of nitric-oxide synthase 2 by aminoguanidine provides neuroprotection of retinal ganglion cells in a rat model of chronic glaucoma. *Proc Natl Acad Sci U S A.* 1999;96(17):9944–9948.
130. Schlamp CL, Johnson EC, Li Y, Morrison JC, Nickells RW. Changes in Thyl gene expression associated with damaged retinal ganglion cells. *Mol Vis.* 2001;7:192–201.
131. Overby DR, Bertrand J, Tektas OY, Boussommier-Calleja A, Schicht M, Ethier CR, Woodward DF, Stamer WD, Lutjen-Drecoll E. Ultrastructural changes associated with dexamethasone-induced ocular hypertension in mice. *Invest Ophthalmol Vis Sci.* 2014;55(8):4922–4933.
132. Whitlock NA, McKnight B, Corcoran KN, Rodriguez LA, Rice DS. Increased intraocular pressure in mice treated with dexamethasone. *Invest Ophthalmol Vis Sci.* 2010;51(12):6496–6503.
133. Shinzato M, Yamashiro Y, Miyara N, Iwamatsu A, Takeuchi K, Umikawa M, Bayarjargal M, Kariya K, Sawaguchi S. Proteomic analysis of the trabecular meshwork of rats in a steroid-induced ocular hypertension model: downregulation of type I collagen C-propeptides. *Ophthalmic Res.* 2007;39(6):330–337.
134. Struebing FL, Geisert EE. What animal models can tell us about glaucoma. *Prog Mol Biol Transl Sci.* 2015;134:365–380.
135. Ishikawa M, Yoshitomi T, Zorumski CF, Izumi Y. Experimentally Induced mammalian models of glaucoma. *Biomed Res Int.* 2015;2015:281214.

136. Morgan JE, Tribble JR. Microbead models in glaucoma. *Exp Eye Res.* 2015;141:9–14.
137. Morrison JC, Cepurna WO, Johnson EC. Modeling glaucoma in rats by sclerosing aqueous outflow pathways to elevate intraocular pressure. *Exp Eye Res.* 2015;141:23–32.
138. McKinnon S, Pease M, WoldeMussie E, Zack D, Quigley H, Kerrigan-Baumrind L, Mitchell R, Ruiz G. Comparison of three models of rat glaucoma caused by chronic intraocular pressure elevation. Bethesda, MD: Association Research Vision Ophthalmology; 1999:S787–S787.
139. Abu-Hassan DW, Li X, Ryan EI, Acott TS, Kelley MJ. Induced pluripotent stem cells restore function in a human cell loss model of open-angle glaucoma. *Stem Cells.* 2015; 33(3):751–761.